AD-A211 124

JMENTATION PAGE

Form Approved
OMB No. 0704-0188

1a. REPORT SECURITY CLASSIFICATION	1b. RESTRICTIVE MARKINGS
UNCLASSIFIED	
2a. SECURITY CLASSIFICATION AUTHORITY	3. DISTRIBUTION / AVAILABILITY OF REPORT
2b. DECLASSIFICATION / DOWNGRADING SCHEDULE	DISTRIBUTION UNLIMITED
4. PERFORMING ORGANIZATION REPORT NUMBER(S)	5. MONITORING ORGANIZATION REPORT NUMBER(S)
FJSRL-JR-87-0012	

6a. NAME OF PERFORMING ORGANIZATION	6b. OFFICE SYMBOL (If applicable)	7a. NAME OF MONITORING ORGANIZATION
Frank J. Seiler Research Lab	FJSRL/NC	

6c. ADDRESS (City, State, and ZIP Code)	7b. ADDRESS (City, State, and ZIP Code)
USAF Academy Colorado 80840-6528	

8a. NAME OF FUNDING / SPONSORING ORGANIZATION AF Office of Scientific Research	8b. OFFICE SYMBOL (If applicable) AFOSR	9. PROCUREMENT INSTRUMENT IDENTIFICATION NUMBER

8c. ADDRESS (City, State, and ZIP Code)	10. SOURCE OF FUNDING NUMBERS			
Bldg 410 Bolling AFB, DC 20332	PROGRAM ELEMENT NO.	PROJECT NO.	TASK NO.	WORK UNIT ACCESSION NO.
	PE62110IF	2303	F2	10

11. TITLE (Include Security Classification)
Nuclear Magnetic Resonance in Molten Salts

12. PERSONAL AUTHOR(S)
John S. Wilkes

13a. TYPE OF REPORT	13b. TIME COVERED	14. DATE OF REPORT (Year, Month, Day)	15. PAGE COUNT
Journal Article	FROM _____ TO _____	87	20

16. SUPPLEMENTARY NOTATION

17. COSATI CODES			18. SUBJECT TERMS (Continue on reverse if necessary and identify by block number)
FIELD	GROUP	SUB-GROUP	
			Thallium 205

19. ABSTRACT (Continue on reverse if necessary and identify by block number)
Nuclear magnetic resonance (NMR) spectroscopy provides information about the structure of molten salts and about interactions among molten salt components. This contribution reviews the application of NMR spectroscopy to molten salts done in this laboratory and by others. The fundamentals of the NMR method are presented, with emphasis on aspects particularly useful to molten salt samples. The limitations to the method resulting from the nature of molten salts and nuclei encountered are discussed. Examples of the types of information about molten salts provided by NMR experiments that are useful to chemists are presented. Chloroaluminate molten salts are the primary melt system used to illustrate the usefulness of NMR spectroscopy. Experiments in organic melts and the use of ^{205}Tl as a probe in nitrates and halides are also treated. Reprints, (AW)

20. DISTRIBUTION / AVAILABILITY OF ABSTRACT	21. ABSTRACT SECURITY CLASSIFICATION
☒ UNCLASSIFIED/UNLIMITED ☐ SAME AS RPT ☐ DTIC USERS	UNCLASSIFIED
22a. NAME OF RESPONSIBLE INDIVIDUAL	22b. TELEPHONE (Include Area Code)	22c. OFFICE SYMBOL
JOHN S. WILKES	(719) 472-2655	FJSRL/NC

DD Form 1473, JUN 86   Previous editions are obsolete.   SECURITY CLASSIFICATION OF THIS PAGE

UNCLASSIFIED

NUCLEAR MAGNETIC RESONANCE IN MOLTEN SALTS

John S. Wilkes
The Frank J. Seiler Research Laboratory
United States Air Force Academy
Colorado Springs, CO   80840
USA

ABSTRACT. Nuclear magnetic resonance (NMR) spectroscopy provides information about the structure of molten salts and about interactions among molten salt components. This contribution reviews the application of NMR spectroscopy to molten salts done in this laboratory and by others. The fundamentals of the NMR method are presented, with emphasis on aspects particularly useful to molten salt samples. The limitations to the method resulting from the nature of molten salts and nuclei encountered are discussed. Examples of the types of information about molten salts provided by NMR experiments that are useful to chemists are presented. Chloroaluminate molten salts are the primary melt system used to illustrate the usefulness of NMR spectroscopy. Experiments in organic melts and the use of ^{205}Tl as a probe in nitrates and halides are also treated.

1.   INTRODUCTION TO THE NMR METHOD

1.1   CW and FT NMR Spectroscopy

    The electromagnetic spectrum spans from acoustic frequencies at the low end to gamma ray frequencies at the high end. In chemistry the range from radio frequencies (about 3×10^6 Hz) to ultraviolet frequencies (3×10^{16} Hz) has been found to be useful. The high energy irradiation available in the ultraviolet provides information about electronic transitions, infrared spectroscopy excites bond vibrations and microwave frequencies are at the energy for rotations and electron spin transitions. Atomic nuclei in a magnetic field will absorb energy in the radio frequency portion of the spectrum. This last phenomenon provides the basis of nuclear magnetic resonance (NMR) spectroscopy, which is a common analytical tool available in most chemical laboratories.
    The fundamental basis of the NMR effect is simple if one uses the simplest of concepts for the atomic nucleus: the spinning charged sphere. In reality, the nucleus is an inhabitant of a world where quantum mechanics governs, so a rigorous explanation of NMR is

217

rather non-intuitive and the arguments can get mathematically abstruse. In this introduction the basic principles of NMR will be outlined and the features of the spectroscopy that provide useful information to molten salt chemists will be presented. This should in no way be considered a complete treatment of NMR principles, but rather a familiarization of the nomenclature and an exposure to the features that reveal chemical information. There are many good texts that provide comprehensive treatments of the material outlined here (1,2).

A spinning charged sphere is a magnetic dipole. In the presence of a magnetic field this magnetic dipole will precess about its spin axis, much like a spinning top in a gravitational field. This precession may be visualized like a mechanical top or, more usefully, as a vector revolving about an axis parallel with the external magnetic field. The length of the vector is the magnetic moment of the nucleus. The "vector representation" of the nucleus will be used here, since it provides the clearest way to understand the interaction of radio frequency radiation with the nucleus.

In a magnetic field of a given strength a nucleus of spin 1/2 can orient in two states. Nuclei with spin other than 1/2 will have more orientations, but for the sake of simplicity the treatment that follows will consider only 1/2 spins. The energy difference between the two orientations is quantized and is proportional to the field strength. It happens that the energy required for the transition corresponds to radio frequencies. The simplest NMR spectrometer would thus consist of a magnet with a sample containing atomic nuclei (i.e., *matter*) *between* its poles, a radio frequency transmitter, and a radio receiver to detect the absorption of energy. This would be a CW (continuous wave) spectrometer, and a recording from the receiver as the transmitter frequency was swept would be an NMR spectrum. In the vector representation of NMR the term resonance refers to the condition when the magnetic vector from the incident radiation is perpendicular to the applied magnetic field (B_O) and is rotating about B_O at the same rate that the nucleus is precessing. This is called the Larmor frequency, ν, given by

$$\nu = |\gamma/2\pi| B_O \tag{1}$$

where γ is the gyromagnetic ratio of the nucleus. To the first order and in the grossest sense, the NMR spectrum depends on one property of the nucleus (γ) and two external forces (from ν and B_O).

For reasons that will be discussed later, not every nucleus with the same γ will resonate at the same frequency, so as the CW spectrometer sweeps in frequency, many resonance lines may be observed. The signal/noise may be improved by collecting information about the nuclear resonance frequencies in the time domain with an FT (Fourier transform) spectrometer. The FT instrument provides a short pulse of radio frequency energy. As the nuclei make their transitions a signal is induced in a receiver that decays with time. The signal, called the FID (free induction decay), contains information about low frequency resonances at early times and higher frequencies at longer times. A Fourier transform of the FID (plus some phase information)

produces a frequency domain spectrum similar to that from a CW
instrument, but having used a "sweep" lasting about a second. The
maximum intensity of the FID occurs when a 90° pulse is used. That
is, the pulse time is precisely long enough to rotate the
magnetization vector 90° from its position at equilibrium in the
rotating frame of reference. If the pulse rotates the magnetization
vector 180°, then no FID is observed, since the decay is along the
z-magnetization axis.

1.2 Relaxation Processes

Observation of the NMR phenomenon requires that a reasonable
portion of the population of nuclei be in the lower energy state at
the beginning. Unlike most electronic transitions, nuclear
transitions to the equilibrium state seldom occur spontaneously. They
require interactions with external fluctuating fields of the
appropriate frequency. This process of interaction with the
environment is called relaxation. Study of the nuclear relaxation can
provide useful information about the surroundings of the nucleus,
i.e., molecules and such. Relaxation times are denoted T_1 and T_2
(spin-lattice and spin-spin), which specify the fundamental relaxation
mechanisms. Frequently relaxation rates ($1/T_1$ and $1/T_2$) are used
instead of relaxation times.

For spin 1/2 nuclei T_1 relaxation is the most important. There
are many mechanisms for T_1 relaxation, the details of which need not
be discussed here. The measurement of T_1 is of interest, since
discussion of some relaxation experiments in molten salts occurs later
in this report. T_1 relaxation of a nucleus to the equilibrium state
occurs exponentially with time. One need only measure the fraction of
nuclei that are still in the non-equilibrium state as a function of
time. The slope of a $\ln(N_\infty - N_t)$ vs time (where N_∞ and N_t are the
fractions magnetized at time=∞ and time=t) will yield T_1. N_∞ and N_t
may be easily measured by a simple sequence of pulses on a FT
spectrometer. A 180° pulse is applied, then after a waiting period t
a 90° pulse is applied. The second pulse "samples" the magnetization
remaining after time=t, which is reflected in the signal intensity
(after transformation). This technique is called the spin inversion
recovery method.

1.3 Chemical Shift

If Equation 1 were the sole determinant of the reson. frequency,
then NMR would be of little interest to chemists. Fortune , the
Larmor frequency of a nucleus is affected by numerous featu. of its
environment. The effect of the local magnetic environment may be
interpreted in terms of molecular or ionic structure, bonding, and
interactions in general.

The chemical shift is actually a rather minor contributor to the
ultimate resonant frequency, but it is the one that provides the most
useful information. Local perturbations to the applied magnetic field
are usually divided into diamagnetic contributions (including chemical

shifts) and paramagnetic contributions (which are usually quite large). Sometimes paramagnetic effects completely mask any effect of chemical shift, such as when conduction electrons are present from metals (the Knight shift). Also, the bulk susceptibility of the medium can greatly affect the resonant frequency. Fortunately, shifts are usually measured against reference materials that are equally affected by the medium.

The source of the chemical shift is electronic shielding. The simplest example of electronic shielding comes from the circulation of s electrons about a nucleus. This generates a local field that opposes the applied field, thus changing the resonant frequency. The local field at atom i will be modified a small amount denoted by the shielding constant, σ_i. Equation 1 becomes

$$\nu_i = |\gamma/2\pi| B_0 (1 - \sigma_i) \tag{2}$$

The chemical shift, denoted δ, is expressed in terms of difference of ν_i from the ν of a reference substance. Since the shielding effect is so small, a factor of 10^6 is applied, and the chemical shift in Equation 3 is in parts per million (ppm).

$$\delta = 10^5 (\nu_{sample} - \nu_{ref.})/\nu_{ref.} \text{ at constant } B_0 \tag{3}$$

The quantity $(\nu_{sample} - \nu_{ref.})$ generally spans the range of 10^{-1} to 10^3 Hz out of a spectrometer frequency of $\sim 10^7$ Hz.

The paramagnetic contribution to chemical shifts has been described in a general theory of magnetic shielding by Ramsey, and results in Equation 4.

$$\delta_p = - \frac{16}{3} \mu_B^2 \left\langle \frac{1}{r^2} \right\rangle \frac{B}{\Delta E} \tag{4}$$

The interesting term in Equation 4 is B. It basically contains information about the interaction of the nucleus with its surroundings. It depends on the coordination number and the orbital overlaps, and is usually interpreted as an indicator of degree of covalency.

1.4 Chemically Exchanging Systems

The frequency of the electromagnetic radiation used in NMR is low compared to that used in most other spectroscopies. In many cases interactions among species containing the nuclei under observation are occurring faster than the time scale defined by the NMR frequency. That case, called the fast exchange limit, is much like photographing a fast event with a camera having a slow shutter speed. An averaged or blurred image results. Valuable information about dynamic processes may be gained from the proper interpretation of the NMR behavior of these systems.

There are three cases that can occur in the NMR of exchanging systems. First, the exchange rate may be slow relative to the

difference in chemical shifts of the two (or more) exchanging
species. This is the slow exchange limit, and one simply sees the
resonances of the separate species. If the exchange rate is very fast
relative to the difference in chemical shifts of the exchanging
species (the fast exchange limit), then only a single line is
observed. The observed shift or frequency is intermediate between
those of the exchanging species, and is determined by the relative
populations of the species. For A and B in fast equilibrium the
observed shift (δ_{obs}) is given by Equation 5,

$$\delta_{obs} = X_A\delta_A + X_B\delta_B \tag{5}$$

where X_A and X_B are the mole fractions of A and B at equilibrium.
     At intermediate rates the analysis of the NMR lines is a little
more difficult. The spectrum may range from two partially merged and
broadened peaks to a single broadened peak. The line shape is
described by the Bloch equations, which basically say that the shape
is proportional to the exchange rate divided by the frequency (or
shift) difference between the species. Line shape simulations using
the function g(ν) in Equation 6 (for two site exchange) are often used
to obtain exchange rates from NMR data.

$$g(\nu) = K\frac{\tau(\nu_A-\nu_B)^2}{[\frac{1}{2}(\nu_A+\nu_B)-\nu]^2 + 4\pi^2\tau^2(\nu_A-\nu)^2(\nu_B-\nu)^2} \tag{6}$$

The quantity K is a normalization constant, τ is the exchange lifetime
and ν_A and ν_B are the resonance frequencies of species A and B.

2. PRACTICAL CONSTRAINTS

2.1 Receptivity

     In order to observe the NMR spectrum of a nucleus in a chemically
interesting situation, there must be sufficient signal from the
spectrometer. The intensity of the NMR response varies over many
orders of magnitude for different nuclei. A useful figure of merit
for NMR response is the receptivity. The receptivity depends on the
gyromagnetic ratio of the nucleus and the abundance of the nucleus.
It is defined as γ^3C, where γ is the magnetogyric ratio and C is the
natural abundance of the nuclide.
     The receptivity relative to a familiar nucleus, such as ^{1}H (D^H) or
^{13}C (D^C) , is the number most often used to gauge the ease of
observation of an unfamiliar nucleus. A relative receptivity near
that of ^{1}H insures that a strong signal will be available (other
things being equal). A relative receptivity near that of ^{13}C will
require many FID accumulations over a considerably longer period of
time. For example, NMR of ^{15}N ($D^C = 2.19 \times 10^{-2}$) is difficult to do,
while ^{205}Tl ($D^C = 7.91 \times 10^2$) is relatively easy. Relative
receptivities are listed in many textbooks and handbooks.

2.2 Quadrupolar Nuclei

Many nuclei do not have 1/2 spins. Those that do not are called
quadrupolar nuclei, and are more complex in their NMR behavior. The
source of the complexity is that the nuclei may have more than two
states in a magnetic field. This provides for a significant
contribution to the T_2 relaxation time. The end result is that the
NMR spectra of quadrupolar nuclei can have broad lines, often many
thousands of Hz wide. If the spectrometer frequency is low and there
is an efficient exchange mechanism operating, then the nucleus may be
unobservable. ^{27}Al is a quadrupolar nucleus and is the predominately
abundant isotope. NMR spectroscopy in molten chloroaluminates must
deal with the quadrupolar effects.

The quadrupolar exchange rate ($1/T_{2Q}$) determines the line width,
and is shown in Equation 7.

$$\frac{1}{T_{2Q}} = \frac{3\pi^2}{10} \frac{2I+3}{I^2(2I+1)} (1 + \frac{\eta_a^2}{3}) \frac{(e^2Qq)^2}{h} \tau_c \qquad (7)$$

The linewidth will depend principally on two properties of the
nucleus (I, the spin and Q, the quadrupole moment) and two features of
the environment (η_a, an asymmetry factor of the surrounding electronic
field and τ_c, the correlation time).

2.3 Magnetic Field

The nature of the magnetic field has a substantial effect on the
quality of the NMR data obtained and the amount of useful information
that may be gained from the spectrum. The three important properties
of the field are strength, homogeneity and stability. The resonance
frequency of a nucleus is directly proportional to the field
strength. An increase in strength has the principal benefit of
improving resolution. Commercial NMR spectrometers have magnets
capable of fields between 1.5 and 12 T. Field strengths above about 2
T are provided by superconducting magnets. Homogeneity of the field
is extremely important due to the very small shifts that are usually
observed relative to the applied frequency. Homogeneity greater than
1 part in 2 X 10^8 is necessary. Stability over long periods of time
is required for long duration data acquisition. This is not difficult
to do if the field/frequency is locked onto a reference resonance.
Stability of greater than 1 part in 1 X 10^9/hr is necessary.

2.4 Temperature

Temperature does not have a major effect on the NMR phenomenon per
se. Temperature does have a number of ancillary effects that affect
the NMR data greatly. Most molten salts are liquid at relatively high
temperatures, so it is common to have to contend with temperature
effects in the study of molten salts by NMR.

The stability of the materials used to construct the probe at high temperature is a major concern. Commercial probes can withstand temperatures up to about 200° C. For temperatures above this, probes are usually custom made.

Temperatures significantly different from the magnet temperature affects the field homogeneity. A high temperature probe must compensate for this effect.

Finally, high temperature can greatly change properties of the sample that in turn affect the NMR behavior. Correlation times are sensitive to absolute viscosity of the sample, which is dependent on temperature. The line shape is sensitive to exchange rate, which is also a function of temperature. Temperature effects on the integrity of the sample, such as vapor pressure and thermal decomposition must be considered when performing NMR experiments at high temperature.

3. CHEMICAL INFORMATION FROM NMR

NMR spectroscopy has been applied to many different classes of molten salts and has provided several types of information about molten salts. This review will concentrate on NMR spectroscopy applied to chloroaluminate melts. The application of NMR to chloroaluminates has some practical advantages, but the primary reason for its emphasis here is that low melting chloroaluminate melts are the principal research interest of the author. Some organic halide melts, inorganic halides and nitrates will also be used to illustrate the usefulness of the NMR method in molten salt chemistry.
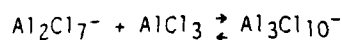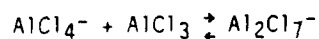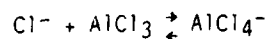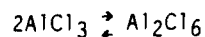
The types of information provided by NMR spectroscopy about molten salts fall into three categories: speciation, interactions and complexation. The NMR data required to provide that information are from chemical shifts, line shape analysis, modeling of exchanging nuclei and analysis of relaxation times.

3.1 Chloroaluminates

As a class of molten salt, chloroaluminates consist of aluminum chloride and some chloride donor. The chloride donor may be an organic chloride salt, in which case the resulting melts often have extraordinarily low melting points. Two such organic chloride salts have been used in recent years: 1-(1-butyl)pyridinium chloride (BuPyCl), which results in a 1-(1-butyl)pyridinium cation (BuPy$^+$) in the melt and 1-methyl-3-ethylimidazolium chloride (MeEtImCl) which results in a 1-methyl-3-ethylimidazolium cation (MeEtIm$^+$) in the melt. More details about these molten salts are presented by other authors participating in this Study Institute.

3.1.1 _Speciation_. The interpretation of NMR data in terms of species is built around the chloroaluminate electrolyte model. That model is a group of equilibria among chloroaluminate anions and $AlCl_3$:

$$2AlCl_3 \rightleftharpoons Al_2Cl_6$$

$$Cl^- + AlCl_3 \rightleftharpoons AlCl_4^-$$

$$AlCl_4^- + AlCl_3 \rightleftharpoons Al_2Cl_7^-$$

$$Al_2Cl_7^- + AlCl_3 \rightleftharpoons Al_3Cl_{10}^-$$

The model predicts that as the composition of the binary melt becomes richer in $AlCl_3$ the anions present will change smoothly from Cl^- to $AlCl_4^-$ to $Al_2Cl_7^-$ as shown in figure 1. ($Al_3Cl_{10}^-$ is not shown in the figure.)

Figure 1. Chloroaluminate Anions.

NMR of ^{27}Al in $AlCl_3$-BuPyCl melts was first reported by Gray and Maciel (3). They observed a single sharp line in basic melts ($AlCl_3 <$ BuPyCl) and a single broad line in acidic melts ($AlCl_3 >$ BuPyCl).

They were able to partially resolve two components of the broad lines
in an acidic melt by raising the temperature (thus reducing viscosity)
and by suppressing the acquisition of low frequency data from the FID
with an extraordinarily long preacquisition delay time. The partially
resolved two line spectrum was presumably due to a narrow line
contribution by $AlCl_4^-$ and a broad line contribution from $Al_2Cl_7^-$.
They calculated a simulated spectrum that closely matched the observed
one, but the fractions of the two components were meaningless due to
the suppression of the broad line intensity.

We performed a more extensive series of ^{27}Al NMR experiments in
$AlCl_3$-MeEtImCl melts (4). With a relatively low field spectrometer we
also observed a single broad line in acidic melt samples. The trick
of using a long preacquisition delay time partially resolved the
spectrum into two lines, one narrow and one broad as seen in figure 2.
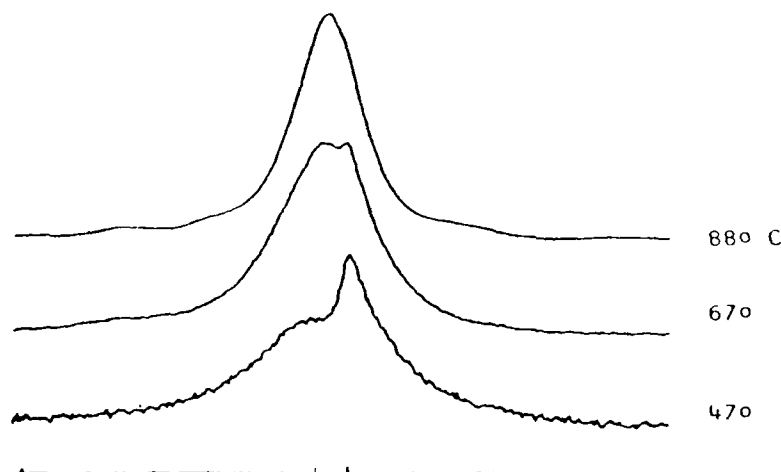

Figure 2. ^{27}Al NMR spectra in $AlCl_3$-MeEtImCl melts.
Melt composition is 0.60 mole fraction $AlCl_3$.

The two site exchange simulations shown in figure 3 reproduce the
experimental spectra quite well. Like the earlier work, we
interpreted the narrow line as evidence for the $AlCl_4^-$ species and the
broad line as the $Al_2Cl_7^-$ species.

The linewidth of the ^{27}Al resonance varied from 140 Hz for a
slightly acidic composition (0.5073 mole fraction $AlCl_3$, "N") to 2170
Hz for a strongly acidic composition (N=0.525). This is to be expec-
ted in light of Equation 7. The situation is complicated by the fact
that the species containing the quadrupolar ^{27}Al and the viscosity are
both changing as a function of composition. The change in species
affects the n_a term in Equation 7 while viscosity controls the
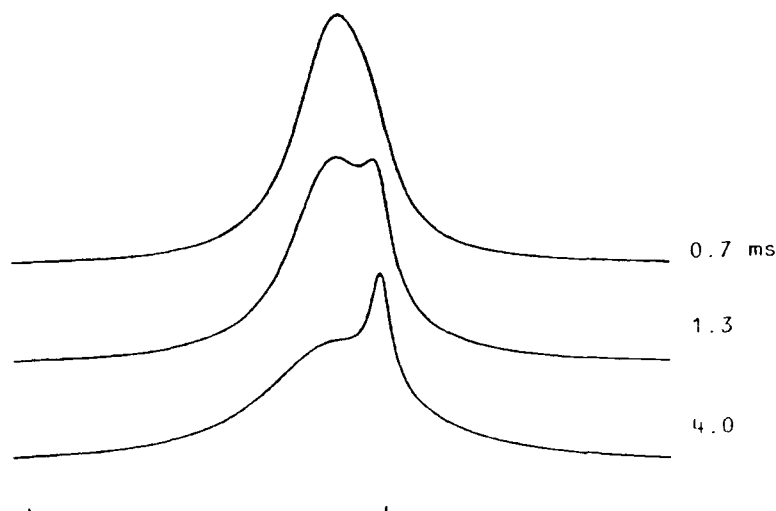correlation time (τ_c). The absolute viscosities of the melts are

Figure 3. Two site exchange simulation of spectra from figure 3.

known as a function of temperature and composition, so the effect of
viscosity may be corrected (τ_C is directly proportional to absolute
viscosity). Figure 4 show, the linewidths corrected for viscosity
plotted as a function of composition. The composition axis in figure
4 is a little unusual. The use of mole fraction $AlCl_4^-$ provides an
axis linear in an anion common to both basic and acidic melts. Note
that in very acidic compositions ($AlCl_4^-$ mole fraction > 0.7) the
widths deviate from the regular trend up to that point. This may
indicate the presence of a new exchanging species in very acidic melts.

The exchange lifetimes (τ) that were entered into the line shape
algorithm are listed in figure 3. A rough activation energy for the
exchange process may be determined from the exchange rate ($1/\tau$)
dependence on temperature. The value is 10 kcal/mol, which is
asgreement with the value of 13 kcal/mol obtained by MNDO calculation
(5) for the process :

$$Al^*Cl_4^- + Al_2Cl_7^- \rightleftharpoons Al^*AlCl_7^- + AlCl_4^-$$

If there is a third exchanging species then the τ values obtained for
two site exchange should be viewed with suspicion.

Further support for the chloroaluminate electrolyte model comes
from ^{27}Al spin-lattice relaxation rate studies in $AlCl_3$–BuPyCl melts
performed by Matsumoto and Ichikawa (6). These workers observe normal
single exponential T_1 decay rates for all basic melts and for melts
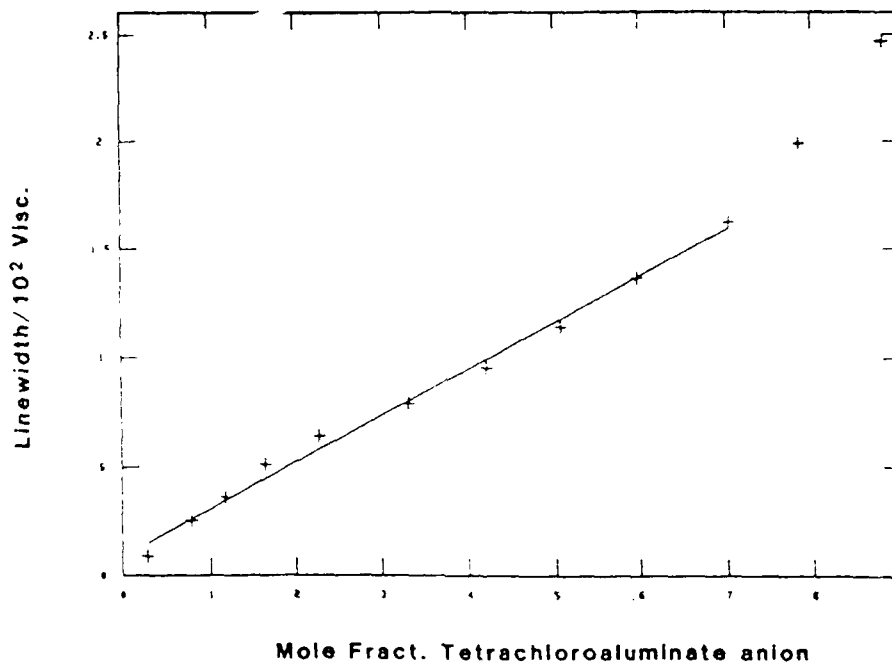having the composition N = 0.5 and 0.67. At all other acidic

Mole Fract. Tetrachloroaluminate anion

Figure 4. ^{27}Al NMR linewidths corrected for viscosity vs composition

compositions the inversion recovery curves appear to be combinations
of at least two exponential decays. The authors interpret these
results as arising from the presence of two species relaxing at
different rates. By curve fitting they were able to estimate the
relative populations of the different relaxing species. The result
was a figure that looks much like figure 1. One very interesting
feature of their study was that they measured the relaxation rates in
melts up to 0.79 mole fraction $AlCl_3$. In these very acidic melts they
claim to see $Al_3Cl_{10}^-$ and Al_2Cl_6.

    In the ^{27}Al studies described so far the presence of two
contributors to the broad line in acidic melts has been inferred from
line shape analysis, relaxation rates or revealed by discarding data
from the broad component of the FID. We have taken ^{27}Al NMR spectra
of $AlCl_3$-MeEtImCl melts at very high field in an attempt to separate
the lines (7). Figure 5 shows the ^{27}Al spectra at different
compositions run in a 500 MHz spectrometer. The basic and neutral
melts show only a single sharp line attributable to $AlCl_4^-$, as seen in
low field spectra. In acidic melts, what was a single line at low
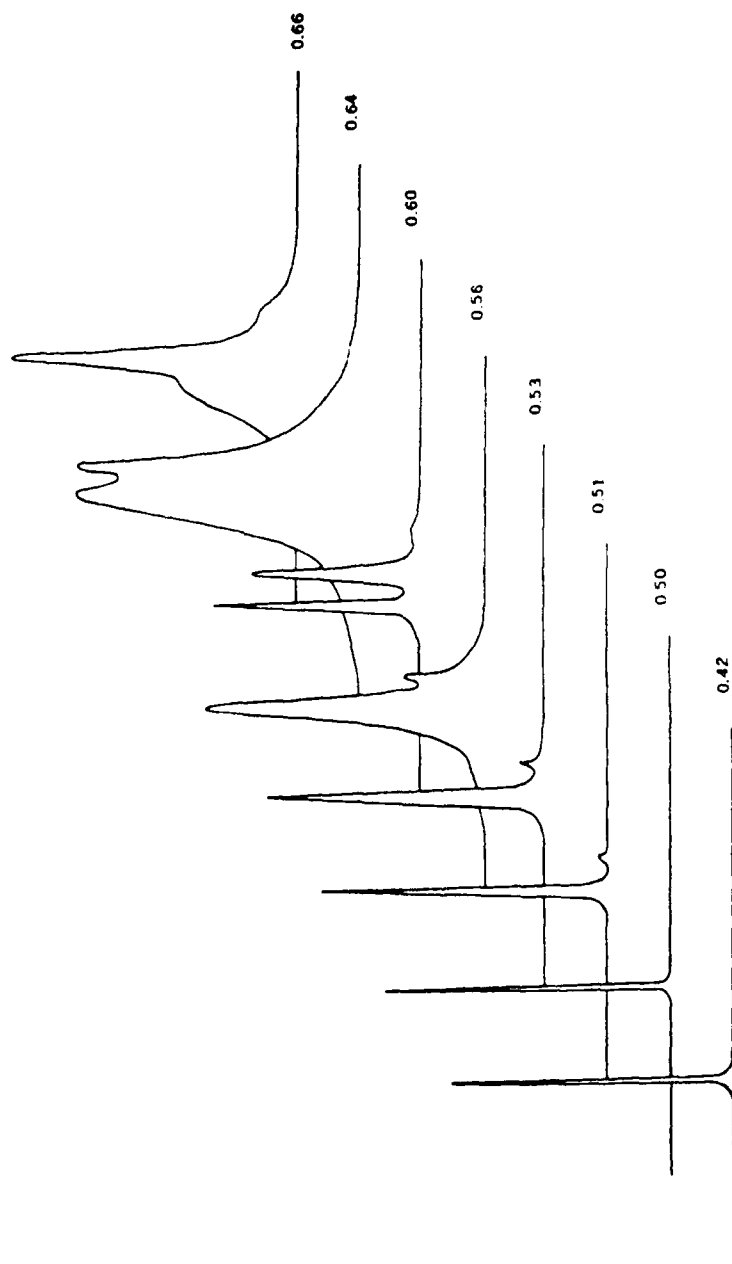field is now resolved into separate lines. As the melt is made

Figure 5. High field ^{27}Al NMR spectra of AlCl$_3$-MeEtImCl melts at 80° C.

0.66

0.64

0.60

0.56

0.53

0.51

0.50

0.42

slightly acidic a additional well resolved line appears due to $Al_2Cl_7^-$. At very acidic compositions a third species is clearly present, probably due to $Al_3Cl_{10}^-$.

^{35}Cl and ^{37}Cl NMR experiments have been attempted in the $AlCl_3$-MeEtImCl melts without success (8). Both isotopes are quadrupolar, the resonant frequencies for both are rather low, and there are undoubtedly numerous efficient exchange mechanisms. All of those factors contribute to an impossibly broadened signal.

3.1.2 Interactions. The organic cation in the $AlCl_3$-BuPyCl and $AlCl_3$-MeEtImCl melts may be seen easily by ^1H and ^{13}C NMR spectroscopy. The first such observations were by Osteryoung and coworkers in the $AlCl_3$-BuPyCl system (9). They compared the ^1H and ^{13}C chemical shifts of nuclei in the $BuPy^+$ ion in acidic chloroaluminate and bromoaluminate melts and concluded that there was no extensive ion pairing. They also studied the effect of addition of benzene to the melt and found that the solvent promoted ion-ion interactions. Osteryoung et al. did not report any results for basic melts, where the effect of composition was later found to be more pronounced.

We have done many ^1H and ^{13}C NMR experiments, primarily in the $AlCl_3$-MeEtImCl melts, in an attempt to understand anion-cation interactions. Figure 6 shows the results of an early experiment that revealed the pronounced difference in the composition dependence of proton chemical shifts between the basic and acidic melts. The signals are sharp and the change in chemical shift in the basic compositions suggests that the chemical shifts are determined by more than one species at the fast exchange limit. The most likely explanation is that the $MeEtIm^+$ ion exchanges among environments that are magnetically distinct and are defined by the nearest neighbor anions to the cations being observed. A relationship like Equation 5 (for two site exchange) or similar (for more than two sites) would apply.

A more detailed analysis of the dependence of chemical shift on melt composition reveals that there are more than two environments for the cation. For basic melts, three magnetically distinct environments may be visualized arising from two nearest neighbor anions that could be both Cl^-, both $AlCl_4^-$ or one of each. Those situations are depicted in figure 7. These species in figure 7 need not be discrete but may be envisaged as portions of oligomeric chains of alternating cations and anions. Simple ion pairs, as suggested by Taulele and Popov (10), are not sufficient to explain the data. The chemical shift resulting from exchange among three environments as in figure 7 is given by

$$\delta_{obs} = \delta_2 Y_1^2 + \delta_{52} Y_1 Y_4 + \delta_8 Y_4^2 \qquad (7)$$

The subscripts associated with each δ denote the magnetic environment for the cation containing the nucleus under observation (vide infra) and Y_1 and Y_4 are ion fraction of Cl^- and $AlCl_4^-$.
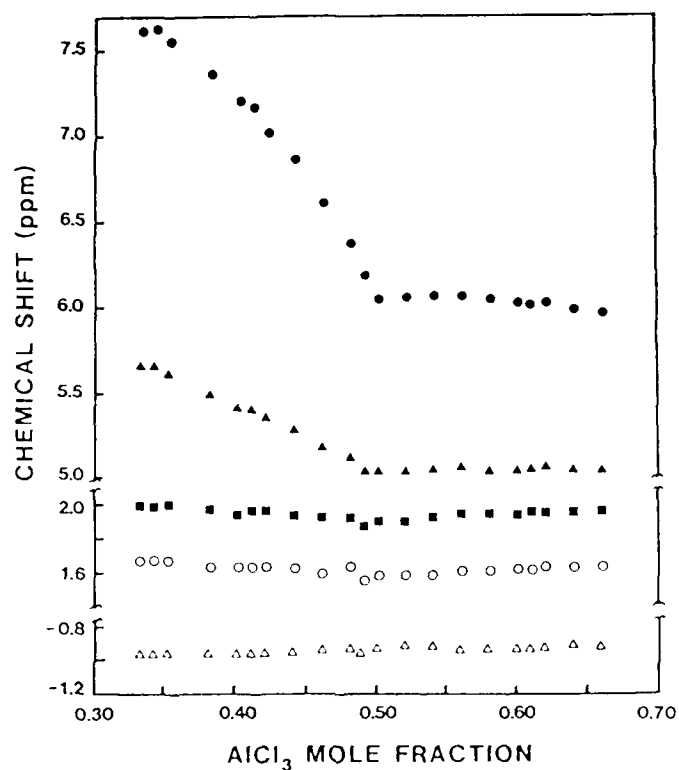
Figure 6. Proton chemical shifts in AlCl₃-MeEtImCl melts.
From top to bottom the data are for H-2 (proton at ring
position 2), H-4&5, N-CH₂, N-CH₃, and CH₃.

$$
\begin{array}{ccc}
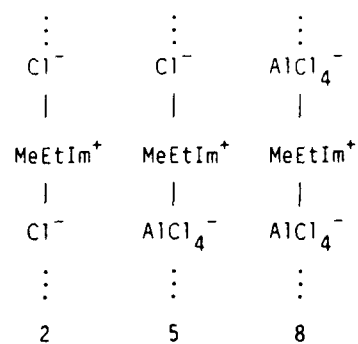\vdots & \vdots & \vdots \\
Cl^- & Cl^- & AlCl_4^- \\
| & | & | \\
MeEtIm^+ & MeEtIm^+ & MeEtIm^+ \\
| & | & | \\
Cl^- & AlCl_4^- & AlCl_4^- \\
\vdots & \vdots & \vdots \\
2 & 5 & 8
\end{array}
$$

Figure 7. Cation environments.

Equation 8 may be restated in terms of Y_4 to give

$$\delta_{obs} = \delta_2 + (2\delta_5 - 2\delta_2)Y_4 + (\delta_8 - 2\delta_5 + \delta_2)Y_4^2 \quad (9)$$

A simple ion pairing model would be linear in Y_4. Figure 8 shows some ^{1}H and ^{13}C data for the entire basic composition range in the $AlCl_3$-MeEtImCl melts. The solid lines are calculated from equation 9 and the dashed lines are for the linear ion pairing model.
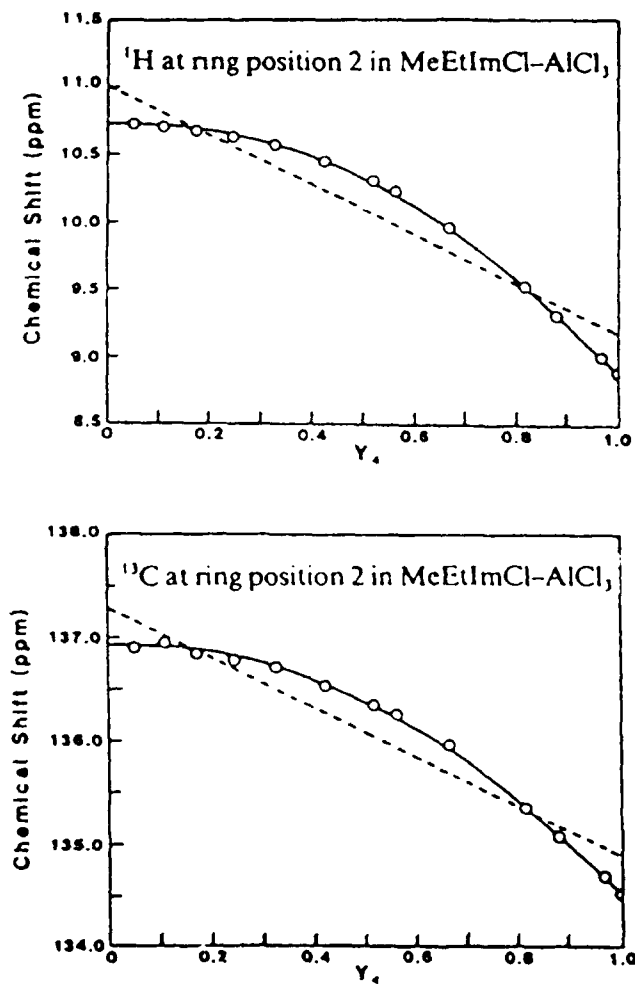

Figure 8.   NMR in $AlCl_3$-MeEtImCl melts.

Melt compositions with the highest proportion of Cl⁻ anions (i.e., the most basic) have chemical shifts that are the most deshielded. This is reasonable, since Cl⁻ is more polarizing than $AlCl_4^-$ and one would expect a greater effect on the MeEtIm⁺ cation.

The addition of a solvent, such as acetonitrile or benzene, to a basic melt has the same effect as removing Cl⁻. Again, this is reasonable due to the mitigation of the interaction between Cl⁻ and MeEtIm⁺ by solvation.

3.1.3 **Complexation**. There is a large body of electrochemical evidence that shows that metal ions are complexed in the room temperature chloroaluminate molten salts. NMR can be used to determine some details about the complexes formed in the melts. Figure 9 shows that when a metal ion is added to a basic $AlCl_3$-MeEtImCl melt, it affects the chemical shift of the MeEtIm⁺ cation. The direction of the change in chemical shifts is as if the metal ion was removing Cl⁻ from the melt. The magnitude of the shift change for a given amount of added metal ion may predicted from the model
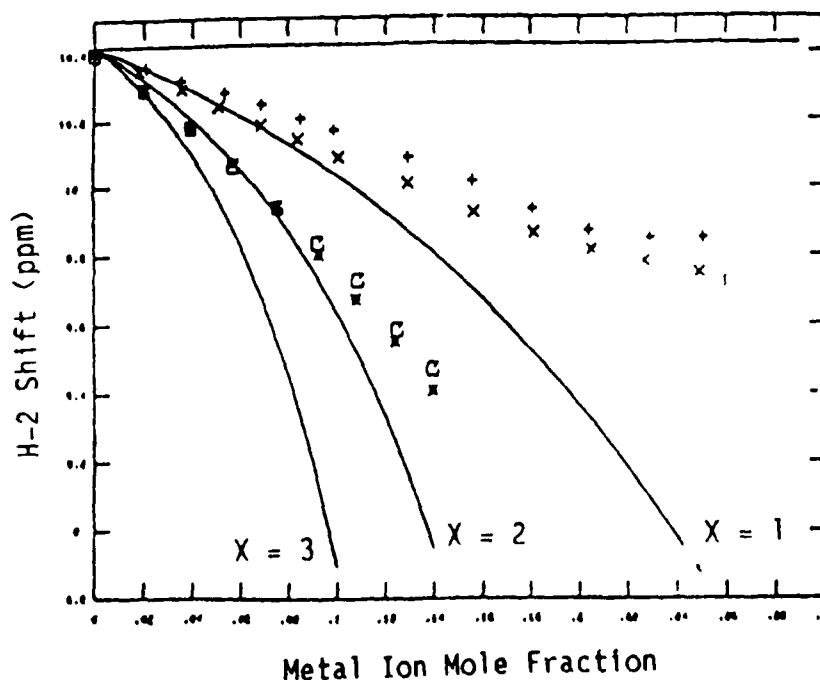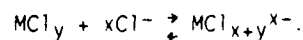

Figure 9. Addition of metal ion chlorides to basic $AlCl_3$-MeEtImCl melt. +=LiCl, X=AgCl, *=CdCl$_2$, □=ZnCl$_2$.

described by Equation 8 (solid lines in figure 9). The effect of the
metal ion will depend primarily on the number of Cl^- (x) consumed by
metal ion M^+ in forming the complex

$$MCl_y + xCl^- \rightleftarrows MCl_{x+y}{}^{x-}.$$

At low concentrations of added metal ion the measured chemical shifts
are as predicted for dichloro (for Li^+ and Ag^+) or tetrachloro (Cd^{2+}
and Zn^{2+}) complexes. The deviations from predicted shifts at higher
metal ion concentrations is almost certainly due to the fact that the
metal ion complex will itself affect the chemical shifts of the
$MeEtIm^+$. A more complex model shown in figure 10 is required to
predict the shifts in the ternary melts.

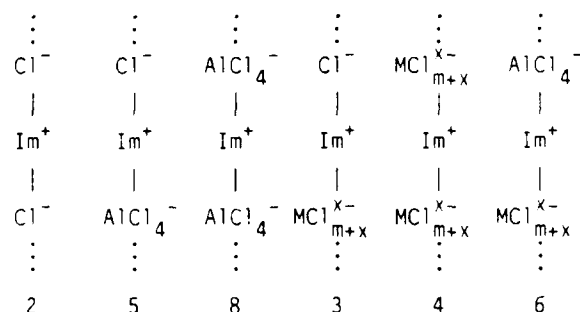| :	:	:	:	:	:
Cl^-	Cl^-	$AlCl_4{}^-$	Cl^-	$MCl_{m+x}{}^{x-}$	$AlCl_4{}^-$
$\|$	$\|$	$\|$	$\|$	$\|$	$\|$
Im^+	Im^+	Im^+	Im^+	Im^+	Im^+
$\|$	$\|$	$\|$	$\|$	$\|$	$\|$
Cl^-	$AlCl_4{}^-$	$AlCl_4{}^-$	$MCl_{m+x}{}^{x-}$	$MCl_{m+x}{}^{x-}$	$MCl_{m+x}{}^{x-}$
:	:	:	:	:	:
2	5	8	3	4	6

Figure 10. Melt model for ternary melts.

The model in figure 10 results in Equation 10:

$$\delta_{obs} = Y_4{}^2(\delta_2 - 2\delta_5 + \delta_8) + Y_4(2\delta_5 - 2\delta_2) + \delta_2 + Y_4 Y_M(2\delta_6 - 2\delta_3 + 2\delta_2 - 2\delta_5)$$

$$+ Y_M(2\delta_3 - 2\delta_2) + Y_M{}^2(\delta_2 + \delta_4 - 2\delta_3) \qquad (10)$$

Y_M is the ion fraction of the metal ion. The δ_i's are obtained by
experiments in $AlCl_3$-MeEtImCl and $AlCl_3$-MCl_y binary melts and by curve
fitting. Figure 11 shows how Equation 9 now fits the data for
$AlCl_3$-MeEtImCl-LiCl ternaries.
    ^{7}Li NMR experiments in $AlCl_3$-BuPyCl-LiCl melts are also consistent
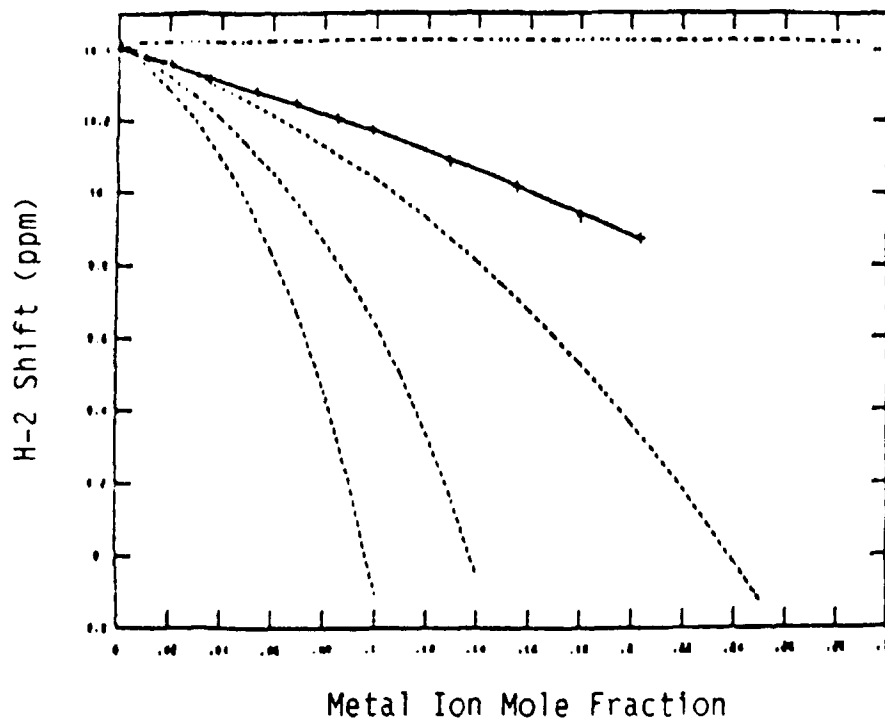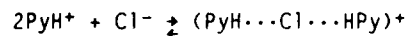with the formation of $LiCl_2{}^-$ (10).

Metal Ion Mole Fraction

Figure 11. ¹H NMR at H-2 in AlCl₃-MeEtImCl-LiCl ternary melts.
Solid line calculated by equation 9 for formation of LiCl₂⁻.

3.2 Organic Halides

¹H NMR has been used by Angell and Shuppert to study the structure
of molten pyridinium chloride (PyHCl)(11). In this melt hydrogen
bonding is possible between the N-H of the pyridine ring and Cl⁻.
AlCl₃ was added to the PyHCl melt to form a series of low melting
binary compositions. The chemical shifts of the ring protons were
found to be sensitive to the mole fraction AlCl₃ in the binaries, with
a sharp change at about the 1:2 AlCl₃:PyHCl composition. The phase
diagram indicated compound formation at that composition. The data
indicate that the PyHCl melt exists as (PyH···Cl···HPy)⁺Cl⁻, and that
AlCl₃ complexes first with the free Cl⁻ then the hydrogen bonded Cl⁻
as more AlCl₃ is added to a binary melt. An estimate of the
equilibrium constant for

$$2PyH^+ + Cl^- \rightleftharpoons (PyH\cdots Cl\cdots HPy)^+$$

was made by using the NMR data to determine the equilibrium amounts of
the PyH$^+$ species. Chemical exchange at the fast exchange limit was
assumed and the chemical shifts were fitted to a two site exchange
model.

A series of molten methylpyridinium halides has been studied by
Newman and coworkers (12). The proton chemical shifts indicated the
presence and absence of hydrogen bonding in various examples of the
melts. The authors were able to correlate the NMR behavior with
transport properties.

3.3 Inorganic Halides

Hafner and Nachtrieb describe the use of ^{205}Tl NMR to determine the
nature of the interactions between cations and chloride and nitrate
anions in Tl containing melts (13). The chemical shifts of thalium
ions are extremely sensitive to short range interactions due to a high
receptivity and the fact that the outer shell electrons are 6s, and
thus easily deformable. The chemical shift for thallous salts can be
more than 10^4 ppm. Nakamura et al. have extended the earlier work in
recent years (14). By relating the observed chemical shifts to
fundamental chemical shift theory (see Equation 4), the authors have
determined cation-anion distances and directly probed the degree of
covalency in thallous halides. In binary thallium halide-alkali
halide melts, the effect of the alkali metal cation on the Tl$^+$-X$^-$ and
Tl$^+$-NO$_3^-$ overlap was revealed. The chemical shifts implied
significant covalent character in some of these melts.

4. REFERENCES

1. High Resolution NMR - Theory and Chemical Applications, E. D.
Becker, Academic Press, 1980.

2. Nuclear Magnetic Resonance Spectroscopy, R. K. Harris, Pitman
Books Ltd., 1983.

3. J. Gray and G. Maciel, J. Am. Chem. Soc., 103, 7147 (1981).

4. J. S. Wilkes, G. F. Reynolds and J. S. Frye, Inorg. Chem., 22,
3870 (1983).

5. L. P. Davis, C. J. Dymek, J. J. P. Stewart, H. J. Clark and W. J.
Lauderdale, J. Am. Chem. Soc., 107, 5041 (1985).

6. T. Matsumoto and K. Ichikawa, J. Am. Chem. Soc., 106, 4316 (1984).

7. L. Dalton and J. Wilkes, unpublished results.

8. J. Wilkes, unpublished results.

9.   J. Robinson, R. C. Bugle, H. L. Chum, D. Koran, and R. A. Osteryoung, <u>J. Am. Chem. Soc.</u>, **101**, 3776 (1979).

10.   F. Taulelle and A. I. Popov, <u>Polyhedron</u>, 889 (1983).

11.   C. A. Angell and J. W. Shuppert, <u>J. Phys. Chem.</u>, **84**, 538 (1980).

12.   D. Newman, R. Rhinebarger, D. Siconolfi and O. Banjoko, <u>J. Electrochem. Soc.</u>, **128**, 2331 (1981).

13.   S. Hafner and N. Nachtrieb, <u>J. Chem. Phys.</u>, **40**, 2891 (1964).

14. Y. Nakamura, Y. Kitazawa, M. Shimoji and S. Shimokawa, <u>J. Phys. Chem.</u>, **87**, 5117 (1983).